2017-04

Comparison Of Potassium And Sodium Binding In Vivo And In Agarose Samples Using Tqtppi Pulse Sequence

Victor D. Schepkin, Andreas Neubauer, Armin M. Nagel and Thomas F. Budinger

The publisher's version of record is available at https://doi.org/10.1016/j.jmr.2017.03.003

Comparison of potassium and sodium binding *in vivo* and in agarose samples using TQTPPI pulse sequence

Victor D. Schepkin[1], Andreas Neubauer[2], Armin M. Nagel[3,4]
Thomas F. Budinger[5]

[1]CIMAR, National High Magnetic Field Laboratory/FSU, Tallahassee, FL, USA
[2]Heidelberg University, Mannheim, Germany
[3]German Cancer Research Center (DKFZ), Heidelberg, Germany
[4]Institute of Radiology, University Hospital Erlangen, Erlangen, Germany
[5]Lawrence Berkeley National Laboratory/UCB, Berkeley, CA, USA

Running title: TQTPPI detection of potassium and sodium

Address for correspondence:
Victor Schepkin, Ph.D.
Research Faculty II
Center for Interdisciplinary Magnetic Resonance
National High Magnetic Field Laboratory
1800 East Paul Dirac Drive
Tallahassee, FL 32310
Tel: 850-645-7357
Fax: 850-644-1366
Email: schepkin@magnet.fsu.edu

Manuscript word count: 5577 words

List of abbreviations:

TQ – triple quantum

SQ – single quantum

MQ – multiple quantum

TPPI – time proportional phase increment

FT – Fourier transformation

RF – radio frequency

TQ^A – TQ MR peak area

SQ^A – SQ MR peak area

A_{SQF} – SQ MR signal amplitude, fast relaxing component

A_{SQL} – SQ MR signal amplitude, slowly relaxing component

A_{SQ} – total SQ MR signal amplitude, sum of the fast and slowly relaxing components

A_{TQ} – TQ MR signal amplitude

T_{2F} – T_2 relaxation time, fast component

T_{2L} – T_2 relaxation time, slow component

t-max – position of the TQ signal maximum

Abstract

Potassium and sodium specific binding *in vivo* were explored at 21.1 T by triple quantum (TQ) magnetic resonance (MR) signals without filtration to achieve high sensitivities and precise quantifications. The pulse sequence used time proportional phase increments (TPPI). During simultaneous phase-time increments, it provided total single quantum (SQ) and TQ MR signals at single and triple quantum frequencies respectively. The detection of both TQ and SQ signals was performed at identical experimental conditions and the resulting TQ signal equals 60 ± 3% of the SQ signal when all ions experience sufficient time for binding. In a rat head *in vivo* the TQ percentage relative to SQ for potassium is 41.5 ± 3% and correspondingly for sodium is 16.1 ± 1%. These percentages were compared to the matching values in agarose samples. The sodium TQ signal in agarose samples decreased in the presence of potassium, suggesting a competitive binding of potassium relative to sodium ions for the same binding sites. The TQTPPI signals correspond to almost two times more effective binding of potassium than sodium. *In vivo*, up to ~69% of total potassium and ~27% of total sodium can be regarded as bound or experiencing an association time in the range of several milliseconds. The analysis of the experimental data indicated that more than half of the *in vivo* total sodium TQ signal could be from extracellular space, which is an important factor for quantification of intracellular MR signals.

Key words: *in vivo*; rat; triple quantum NMR; potassium; sodium; binding; TQTPPI;

Introduction

Potassium and sodium are major ions *in vivo* and their MR signals have great potential to convey valuable information about cell functioning (1-5). The difference in concentration of potassium and sodium between intracellular and extracellular sites is an important indicator of cellular energy metabolism (6-8).

In addition to *in vivo* studies of the single quantum (SQ) signals from sodium in brain and heart, the triple quantum (TQ) MR signals from sodium and potassium have come under investigation (9-18) because of their potential to reveal changes in intracellular ion content without using contrast agents. For example, after calibration, the TQ filtered (TQF) sodium MR signal can measure changes in the intracellular sodium concentration in an isolated perfused rat heart without shift reagents (19). TQ signals are a typical features *in vivo* MR of potassium and sodium nuclei, as they both have spin S = 3/2. These ions interact with the surrounding electric field gradients of the macromolecules *in vivo* and the corresponding quadruple interactions are usually very small ($<$ 200 Hz), and their effect cannot be observed as separate satellite MR peaks. However, there are exceptions as was observed for potassium in muscle (20), sodium in cartilage (21) and the optic nerve (22). *In vivo* the macromolecules are mainly proteins and the binding time in the range of several milliseconds results in a TQ MR signal.

A widespread and accurate use of TQ signals is currently hindered by the low intensity of NMR signals, for example, potassium, and by the presence of residual MR signals routinely observed during TQ filtration. Historically, the application of TQF pulse sequences was the primary way to detect TQ signals. TQF detection is usually performed by pulse sequence 90 -τ- 90-δ-90 (Fig. 1) using a specially selected phase cycling. The TQF pulse sequence interval "τ" is usually maximized for the most prevailing time of binding out of the wide range of ion binding existing *in-vivo*; a typical value for interval "τ" is ~2-6 ms. Other types of both stronger and weaker binding are not optimally detected. The TQF signal *in-vivo*, detected by such pulse sequences is only a small fraction of the total single quantum (SQ) signal.

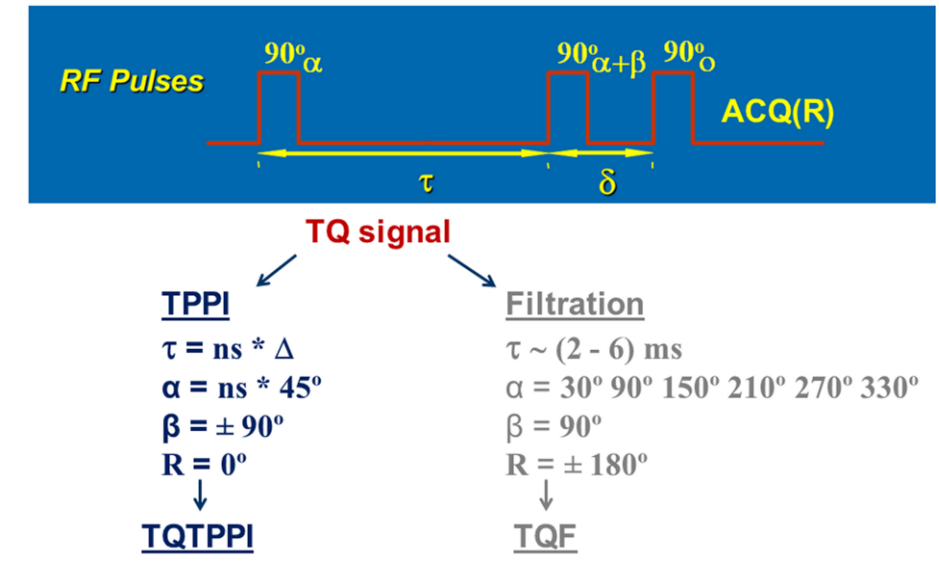

Fig. 1. *Comparison of the TQTPPI and TQF pulse sequences. The TQTPPI pulse sequence has simultaneous increments of interval τ = ns*Δ and RF phase α = ns*45°. The RF phase β has values of +90° and -90° for each value of τ and α and both results are added together to suppress a double quantum signal. The receiver phase R remains unchanged. In the TQF pulse sequence, the interval "τ" has a fixed value in the range of 2 – 6 ms. The phase α changes throughout the cycle of 6 steps, while the receiver phase alternates ± 180° with each RF phase step. A sum of all signals gives the TQF signal. A 180 degree pulse (180 $_{\alpha+90°}$) at the middle of interval "τ" is not shown.*

A dramatic improvement in the efficiency and accuracy of the TQ signal detection can be achieved by avoiding filtration using the TQTPPI method (Fig. 1). In comparison to a typical TPPI pulse sequence (23,24), where the phase increment is 90º, the largest phase increment to detect the TQ signal is 45º. Smaller phase steps are also acceptable, for example 30º. The TQTPPI has a comparable efficiency for a wide range of ion bindings. The TQ MR signals are acquired concurrently with SQ peak. For example, during 45º phase increment a full cycle is covered by 8 phase steps. Thus, after Fourier transform (FT) in second dimension, the SQ peak can be found at 1/(8*$\Delta\tau$), which is well separated in a frequency domain from the TQ signal at 3/(8*$\Delta\tau$).

The TQTPPI pulse sequence for sodium was previously shown in the test samples (25,26) and *in vivo* (27). The current study is devoted to the application and analysis of the TQTPPI pulse sequence for potassium and sodium in a rat head at 21.1

T. The results were compared with the corresponding data from TQF experiments. Additionally the same experiments were conducted in the model system containing 7.5% agarose. This concentration of agarose gives the MR relaxation parameters close to the *in vivo* results (28). The model system was able to demonstrate a stronger and competitive binding of potassium relative to sodium for the same binding places.

Methods

The experiments were performed on a 21.1T magnet using Bruker MRI Avance III console (PV 5.1) and 64 mm gradient coil (RR, Inc.). Volume MRI coils for potassium (41.8 MHz) and sodium (^{23}Na, 238 MHz) were approximately the same size with ID/L = 33/54 mm. A double tuned Na/H RF coil was described previously (29). The potassium coil was a single tuned RF coil of Alderman-Grant design (28).

A commonly used TQ filtering pulse sequence $90^{o}_{\alpha} - \tau - 90^{o}_{\alpha+\beta}$ -δ- 90^{o}_{0} was modified so that the phase "α" was incremented by 45º (α = ns*45º), at each step ns when the time delay (τ = ns*Δ) was incremented (Fig. 1). Before incrementing τ the phase "β" was alternated (± 90º) and the results were added to suppress the double quantum (DQ) signal. The interval δ is usually selected to be the minimum allowed by the MR scanner hardware (~ 100 μs). The time increment Δ in TQTPPI pulse sequence was 100 - 300 μs, the typical durations of the 90º pulse for sodium was 120 μs, and 140 μs for potassium. In both pulse sequences, TQTPPI and TQF, a $180^{o}_{\alpha+90}$ pulse was used in the middle of "τ" interval to compensate for the inhomogeneity of the magnetic field.

Free induction decays were acquired with "np" complex points, for potassium np = 2048, and for sodium np = 4092. Number of increments "ns" was selected in the range 128 - 1024. The large numbers of steps (>128) were selected to increase accuracy of the spectra in the second dimension in some experiments. The spectral width was 25 KHz for potassium and sodium. Number of accumulations NA and repetition time TR were for potassium NA = 16, TR = 200 ms, for sodium NA = 1 and TR = 300 ms. The FID signals were phased and Fourier transformed (FT) in the first dimension. Then "ns" data points at the position of (np/2 + 1) in these spectra were selected, i.e. it was at the maximum of the central peaks. These points were used for a

nonlinear fit in the time domain to derive amplitudes of the SQ and TQ signals. The same data were also FT transformed in the second dimension using the TPPI mode in which the phased real part was accompanied by zero filling for the omitted imaginary points. The area of the SQ signal and both positive and negative parts of the TQ peak areas were calculated. The SQ peak was normalized to 100%. Pre-processing of the above and other data was performed using MatNMR software v.3.9.94 (30). All results are presented as mean ± standard deviation.

The pulse sequence was first tested using samples with agarose gel 5% and 7.5% containing NaCl or KCl (154 mM). A competition between K^+ and Na^+ ions was observed when both NaCl (154 mM) and KCl (154 mM) were added to the agarose samples at the same time. The agarose (Carl Roth, Karlsruhe, Germany) was dissolved in the above solutions and heated up to 90°C with stirring. All samples had been placed to the same plastic cylindrical container (diameter = 27 mm and length = 60 mm; volume = 25 mL).

The TQTPPI potassium MRI signals were also acquired from polycrystalline potassium chloride (KCl). The results served as a reference emulating a 100% binding of potassium. In this specific case of a solid sample, a 180 degree pulse at the middle of "τ" interval was not used.

The TQTPPI/TQF pulse sequences were applied to detect potassium and sodium TQ signals in five male Fisher 344 rats (weight ~ 200 g). The animals were anesthetized by breathing a 1.5% v/v isoflurane/air gas mixture. The rat head was reproducibly positioned in the RF coil to within ± 1 mm using a bite bar (29). The TQ signal maximum amplitude and its position t-max were calculated using a time fit of the TQ two-exponential decay.

All animal experiments were conducted according to the protocols approved by The Florida State University ACUC.

Results

Comparison of potassium and sodium TQTPPI and TQF MR signals

One way to process the TQTPPI data is to perform a non-linear fit of the total TQTPPI signal (Fig. 2) using the fitting function (31):

$$Y = A_{SQL}\sin(\omega t)\exp(-t/T_{2L}) + A_{SQF}\sin(\omega t)\exp(-t/T_{2F}) + A_{TQ}\sin(3\omega t)(\exp(-t/T_{2L})-\exp(-t/T_{2F})) + DC \quad (3)$$

- where Y - amplitude of the fid signal, t - time, ω- frequency of the phase modulation = 1/(8*Δ), Δ - time step increment, DC is a base line shift, containing imperfect settings of the RF pulse durations and the accuracy of the phase corrections.

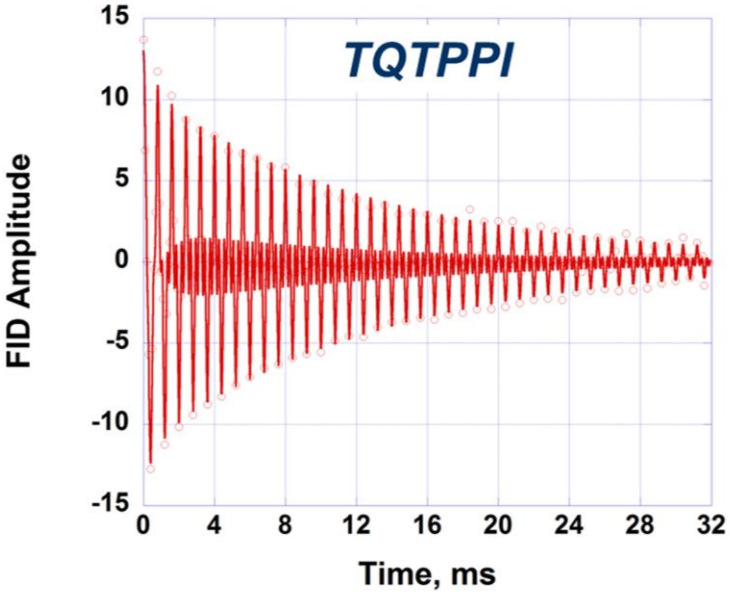

Fig. 2. *Time course of potassium TQTPPI MR magnetization from a rat head in the second dimension. It is noticeable, that the TQ MR signal of potassium appears quickly near the base line and slowly decays later on.*

The parameters of the time domain fit of the TQTPPI signals from the rat head as well as a corresponding TQF results are presented in Table 1. It is important to note that single quantum signal has two exponential relaxation components (Fig. 3).

Table 1. *In vivo potassium and sodium TQ MR signal parameters in the rat head. Note a less efficient sodium binding and the similarity of the TQTPPI and TQF parameters.*

TQ parameters	Potassium TQTPPI	Potassium TQF	Sodium TQTPPI	Sodium TQF
TQ^A/SQ^A, %	41.5 ± 3		16.1 ± 1	
A_{TQ}/A_{SQ}, %	35.7 ± 2.8		15.4 ± 1	
A_{SQF}/A_{SQ}, %	55.3 ± 0.9		41.6 ± 0.9	
T_{2L}, ms	13.3 ± 0.4	13.8 ± 0.8	30.6 ± 2	28.9 ± 1
T_{2F}, ms	0.79 ± 0.03	0.85 ± 0.14	2.3 ± 0.2	2.2 ± 0.5
t-max, ms	2.37 ± 0.07	2.5 ± 0.3	6.5 ± 0.6	6.0 ± 0.9

- TQ^A/SQ^A - ratio for the TQ peak area to the SQ peak area in the TQTPPI spectrum. A_{SQ} - total SQ signal amplitude, $A_{SQ} = A_{SQL} + A_{SQF}$; A_{TQ} – TQ signal amplitude (A_{SQL}, A_{SQF} and A_{TQ} are from TQTPPI time domain fit, formula (3)). T_{2L} and T_{2F} are slow and fast components of the bi-exponential relaxation of the SQ and TQ signals, t-max is a time position of the TQ signal maximum.

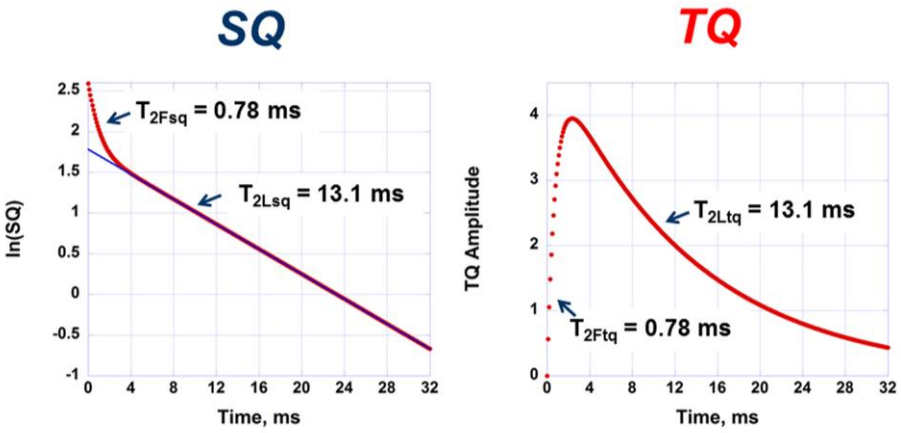

Fig. 3. *The results of non-linear fit in the time domain of potassium TQTPPI magnetization from the rat head (from Fig. 3). Note the two-exponential decay for the SQ signal, which represents a total MR potassium signal from a rat head.*

The other way to process the TQTPPI data is to perform Fourier transformation in the second dimension of the TQTPPI data (Fig. 4). The results are demonstrated for potassium and sodium in a normal rat head from *in vivo* studies (Fig. 4). The sodium

SQ peak and the TQ peak are well separated having frequencies of 1.25 kHz or 1/(8*Δ) and 3.75 kHz or 3/(8*Δ) respectively. The TQ peak areas relative to the corresponding SQ peak areas (TQ^A/SQ^A) were 41.5 ± 3% for potassium and 16.1 ± 1% for sodium.

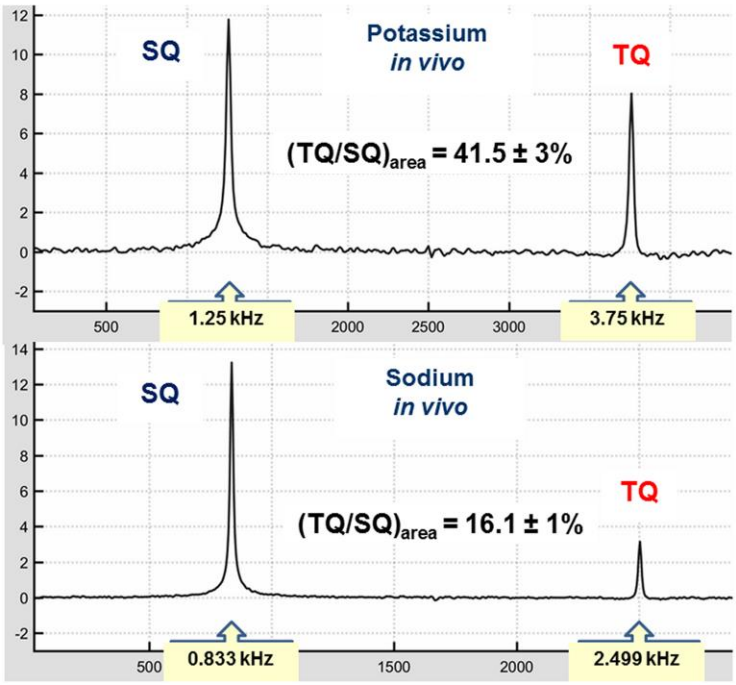

Fig. 4. *TQTPPI spectra for potassium (Δ = 0.1 ms, ns = 320, scan time = 30 min) and sodium (Δ = 0.15 ms, ns = 760, scan time = 7 min) in the rat head at 21.1T. The percentages (TQ^A/SQ^A) peak area for potassium was 41.5 ± 3%, and for sodium 16.1 ± 1%.*

It is important to note that SQ MR signal represents a total MR signal, that is, both the bound and free ions of potassium and sodium. In contrast, the TQ signal represents only specifically bound ions.

For comparison, in the saline solution (0.9% NaCl), the TQTPPI pulse sequence does not give a sodium TQ signal. The base line at the expected place for the TQ signal is very clean up to the noise level. Another example of the absence of a TQ signal is during sodium binding to glycerol. No TQ signal was detected despite that the fact that binding of sodium to the glycerol molecule can shorten sodium MR relaxation times T_1 and T_2 up to 8 ms.

For quantification of the level of binding, solid polycrystalline KCl was used, because all potassium ions are in a bound state. The defects in the crystals are usually

enough to produce small quadrupole interactions at the position of potassium, which are fixed due to the limited mobility of potassium in the crystal. The TQTPPI spectrum gives the TQ peak area of 59.9 ± 3% (n = 6) relative to the SQ peak area (Fig. 5). This percentage is very close to a theoretical expectation for the intensity of the satellite transitions 1/2 <-> 3/2 of 60% (32,33).

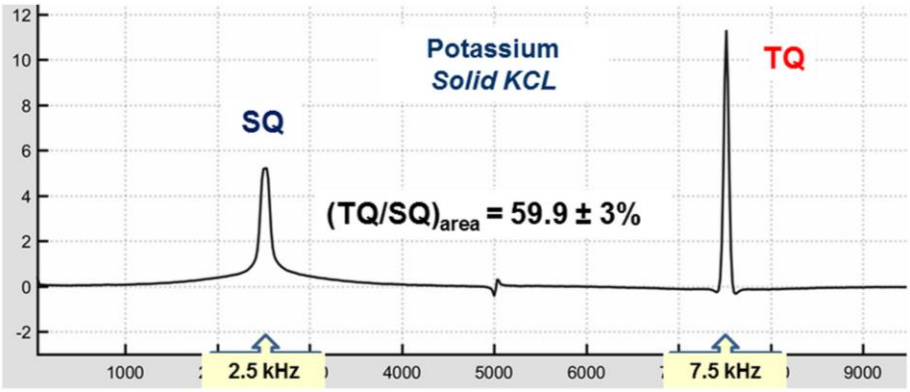

Fig. 5. *Potassium TQTPPI spectrum from polycrystalline KCL serves as a reference for the one hundred percent bound potassium system with (TQ^A/SQ^A) peak area's ratio of 59.9 ± 3% (Δ = 0.05 ms, ns = 400, TR=30 sec, scan time = 6.5 h). Thus, the TQ signal in the TQTPPI pulse sequence represents the intensity of the MR quadrupole satellite transitions.*

The comparison of potassium and sodium binding was also performed in the test samples containing 5% and 7.5% agarose with 154 mM KCl or 154 mM NaCl (Table 2). The percentages of the peak areas of TQ signal to SQ signal for potassium alone was 33.5 ± 0.1% (n = 3) in 5% agarose and increasing to 45.8 ± 1% (n = 3) in 7.5% agarose. The corresponding value for sodium were 25.7 ± 0.7% (n = 4) and 27.3 ± 0.3% (n = 4). The other parameters of the TQTPPI time domain fit are presented in Table 2.

Table 2. *TQTPPI detection of the competitive potassium binding over sodium for the same binding places in 5% (A) and 7.5% agarose (B). Note a decrease of sodium TQ signal in the presence of potassium in both cases:*

Table 2A. *TQTPPI, Agarose 5%*

Potassium	KCl (154 mM)	KCl(154 mM)+NaCl(154 mM)
$(TQ^A/SQ^A)_K$, %	33.5 ± 0.1	33.9 ± 0.9
$(A_{TQ}/A_{SQ})_K$, %	32.5 ± 0.3	33.3 ± 0.6
$(A_{SQF}/A_{SQ})_K$,%	58.9 ± 0.4	58.3 ± 0.2
$T_{2L\,K}$, ms	25.3 ± 0.4	23.8 ± 1
$T_{2F\,K}$, ms	1.96 ± 0.1	1.8 ± 0.3
t-max $_K$, ms	5.4 ± 0.1	5.0 ± 0.3
Sodium	NaCl (154 mM)	NaCl(154 mM)+KCl(154 mM)
$(TQ^A/SQ^A)_{Na}$, %	25.7 ± 0.7	20.3 ± 0.7 *
$(A_{TQ}/A_{SQ})_{Na}$, %	25.3 ± 0.6	21.7 ± 0.7 *
$(A_{SQF}/A_{SQ})_{Na}$,%	61 ± 0.5	60.2 ± 1
$T_{2L\,Na}$, ms	42.1 ± 0.9	43.4 ± 1.7
$T_{2F\,Na}$, ms	5.0 ± 0.1	6.6 ± 0.4 *
t-max $_{Na}$, ms	12.2 ± 0.2	14.7 ± 0.8 *

Table 2B. *TQTPPI, Agarose 7.5%*

Potassium	KCl (154 mM)	KCl(154 mM)+NaCl(154 mM)
$(TQ^A/SQ^A)_K$, %	45.8 ± 0.9	47.4 ± 1.3
$(A_{TQ}/A_{SQ})_K$, %	42.4 ± 0.5	44.5 ± 1.5
$(A_{SQF}/A_{SQ})_K$,%	57.8 ± 0.9	57.2 ± 1.4
$T_{2L\,K}$, ms	14.5 ± 0.5	13.5 ± 1.3
$T_{2F\,K}$, ms	1.2 ± 0.1	1.07 ± 0.1
t-max $_K$, ms	3.3 ± 0.1	2.9 ± 0.1
Sodium	NaCl (154 mM)	NaCl(154 mM)+KCl(154 mM)
$(TQ^A/SQ^A)_{Na}$, %	27.3 ± 0.3	22.3 ± 0.7 *
$(A_{TQ}/A_{SQ})_{Na}$, %	25.0 ± 0.4	22.3 ± 0.7 *
$(A_{SQF}/A_{SQ})_{Na}$,%	61.1 ± 0.5	61.2 ± 0.7
$T_{2L\,Na}$, ms	36.4 ± 2.5	37.4 ± 3.8
$T_{2F\,Na}$, ms	3.9 ± 0.2	4.9 ± 0.4 *
t-max $_{Na}$, ms	9.7 ± 0.6	11.4 ± 1 *

*- $(TQ^A/SQ^A)_K$, $(TQ^A/SQ^A)_{Na}$ - ratios for the TQ peak area to the SQ peak area in the TQTPPI spectrum for potassium and sodium signals respectively. A_{SQ} - total SQ signal amplitude, $A_{SQ} = A_{SQL} + A_{SQF}$; A_{TQ} – TQ signal amplitude (A_{SQL}, A_{SQF} and A_{TQ} are from TQTPPI time domain fit, formula (3)). T_{2L} and T_{2F} are slow and fast components of the bi-exponential relaxation of the SQ and TQ signals, t-max is a time position of the TQ signal maximum. * - difference is statistically significant.*

The process of competition between potassium and sodium was detected by TQTPPI method when both KCl and NaCl were simultaneously present with the same concentration of 154 mM. At both concentrations of agarose, the TQ signal for sodium decreased significantly in the presence of potassium (Table 2). For the agarose concentration of 5%, the sodium TQ peak area signal decreased from 25.7 ± 0.7% (n = 4) to 20.3 ± 0.7% (n = 6). In the samples having 7.5% agarose, the corresponding decrease of sodium TQ signals is from 27.3 ± 0.3% (n = 4) to 22.3 ± 0.7% (n = 3).

These changes correlate with an increase of the sodium fast relaxing component $T_{2F\,Na}$ in the presence of potassium from 5.0 ± 0.1 ms (n = 4) to 6.6 ± 0.4 ms (n = 6) for 5% agarose samples and from 3.9 ± 0.2 ms (n = 4) to 4.9 ± 0.4 ms (n = 3) for 7.5%

agarose samples. The consistent increase is also observed for the position of sodium TQ signal maximum in the presence of potassium from 12.2 ± 0.2 ms (n = 4) to 14.7 ± 0.8 ms (n = 6) for 5% agarose samples. In the samples with 7.5% agarose the corresponding increase is from 9.7 ± 0.6 ms (n = 4) to 11.4 ± 1 ms (n = 3) (Table 2).

Discussion

The polycrystalline KCl was selected to serve as a reference system where all potassium ions are bound. The application of the TQTPPI pulse sequence (Fig. 5) demonstrates that the experimental TQ peak area is very close to the theoretically expected value of 60% of the SQ peak area (32,33). Thus, empirically, the observed TQ signal in the TQTPPI pulse sequence represents the intensity of the quadrupole satellite transitions.

It is expected that small quadruple interactions can decrease the intensity of the SQ peak signal (Fig. 5). In the TQTPPI sequence the same SQ signal is used to detect both SQ and TQ signal in the second dimension. Thus, the ratio of the TQ/SQ signals will represent the intensity of the satellite transition with a good accuracy.

Using the above result for polycrystalline KCl (Fig. 5) as a model for 100% binding, we can estimate from Table 1 that *in vivo* in the rat head approximately 41.5x100/60 = 69% of total potassium has long term binding. The corresponding data for sodium *in vivo* suggests that much less, approximately 27%, of sodium has long term binding.

The large difference in the relative TQ signal intensity between potassium and sodium raises a question if this is relevant to the predominant intracellular location of potassium. In efforts to find the answer, the TQTPPI signals of potassium and sodium were compared in the test samples containing 5% and 7.5% agarose (Table 2). The results of experiments, first of all, demonstrate that potassium, at the same binding places, gives a larger TQ/SQ ratio than sodium. In 5% agarose the percentage of TQ peak area relative to the SQ peak area for potassium $(TQ^A/SQ^A)_K$ = 33.5%, while that for sodium $(TQ^A/SQ^A)_{Na}$ = 25.7%. The results for 7.5% agarose show for potassium $(TQ^A/SQ^A)_K$ = 45.7% and for sodium $(TQ^A/SQ^A)_{Na}$ = 27.3%. Thus both results *in vivo* and in the agarose samples indicate that potassium has a stronger TQ signal than sodium indicating of a stronger binding of potassium.

TQTPPI experiments offer additional and more direct evidence that potassium has stronger binding. Potassium can compete with sodium for the binding places as observed when both potassium and sodium were added together (Table 2). The results demonstrate that there is practically no change in potassium binding in the presence of sodium. For example, in the presence of sodium or without it, the percentage of the TQ peak area relative to the SQ peak area $(TQ^A/SQ^A)_K$ for potassium remains at the same level of 33.7% for the 5% agarose sample and at a level of 46.5% for the 7.5% agarose sample. However, the TQ signal of sodium is decreased in presence of potassium. The TQ peak area relative to SQ peak area for sodium $(TQ^A/SQ^A)_{Na}$ decreased from 25.7 ± 0.7% to 20.3 ± 0.7% for the 5% agarose samples in the presence of potassium and from 27.3 ± 0.3% to 22.3 ± 0.7% for the 7.5% agarose. Thus, it appears that potassium binding competes with bound sodium. These results correlate with experiments of others on changes of sodium T_1 relaxation times in the presence of phosphatidylserine vesicles due to the partial displacement of sodium by potassium (34). The preference of potassium binding over sodium was also detected in rat liver cell microsomes (35).

It is important to note that there is a difference for potassium between the ratio of the peak areas (TQ^A/SQ^A) and ratio for the amplitudes (A_{TQ}/A_{SQ}) obtained from the time domain fit (Eq. 3) of the results of TQTPPI pulse sequence (Table 1). However, there is almost no such difference of these ratios for sodium. These results suggest that the two exponential fit of the TQ signal is only a first order of approximation. It is working for sodium and approximately for potassium in 5% agarose samples (Table 2A) and for sodium *in vivo* (Table 1). In all other cases the deviation between (TQ^A/SQ^A) and (A_{TQ}/A_{SQ}) can be observed suggesting more than two or a distribution of the T_2 relaxation times for bound ions.

Another important observation is that the fast decaying components of the SQ signal $(A_{SQF}/A_{SQ})_K$ and $(A_{SQF}/A_{SQ})_{Na}$ in the TQTPPI pulse sequence are of 57 - 61% for agarose samples (Table 2). These values are very close to a theoretical expectation of 60% for the intensity of the MR satellite peaks during quadrupole interaction. However, as it can be seen in the Table 2, the TQ signals in both cases are much less than 60%, the expected value if all of ions experience quadrupole interaction. Thus, a short component of the SQ signal includes both ions with long time binding, represented by

TQ signal and by ions bound to small molecules which may not yield contribution to the TQ signal.

In vivo, in the rat head, the A_{SQF}/A_{SQ} values are much smaller for sodium; it is 41.6%, and it is a little less for potassium at 55.3% (Table 1). A value below 60% could be an indication that *in vivo*, a large fraction of sodium and a small fraction of potassium are in a "free" state, i.e. not experiencing significant long time quadrupole interactions.

Estimation of sodium intracellular and extracellular TQ signals

Using the above results for potassium and sodium TQ signals, an estimation of the TQ signals which could come from *in vivo* intracellular and extracellular spaces can be made. The intracellular volume is estimated at 0.85 of total tissue volume and sodium intracellular and extracellular concentrations are 15 mM and 140 mM, respectively, which is close to estimations of others (36). In this case intracellular sodium content could be $0.378*Na_T$, and extracellular sodium content is $0.622*Na_T$, where Na_T is a total sodium content in tissue. The difference between sodium and potassium TQ signals can be taken from the TQTPPI results in samples with 7.5% agarose (Table 2). These samples have T_1, T_2 MR relaxation parameters very close to sodium and potassium *in vivo* (28). Thus, from Table 2 sodium has 47.4/22.3 = 2.1 times less TQ signal than potassium. The intracellular potassium TQ signal can be with high accuracy presented by potassium $(TQ^A/SQ^A)_K$ = 41.5% (Table 1) as only ~ 0.4% of potassium in the normal state is in extracellular space. From here it can be estimated that for intracellular sodium $(TQ^A/SQ^A)_{Nai}$ = 41.5/2.1 = 19.8%. Assuming that total $(TQ^A/SQ^A)_{Na}$ signal in rat head of 16.1 % is composed from extracellular and intracellular contribution we will have

$$0.378*(TQ^A/SQ^A)_{Nai} + 0.622*(TQ^A/SQ^A)_{Naex} = 16.1 \qquad (4)$$

From this equation for extracellular sodium $(TQ^A/SQ^A)_{Naex}$ = 13.9%. Consequently, TQ binding of sodium in intracellular space is stronger $(TQ^A/SQ^A)_{Nai}$ $/(TQ^A/SQ^A)_{Naex}$ = 19.8/13.9 = 1.4.

Thus, the total TQ_i^{Na} signal of sodium in intracellular space and extracellular spaces are

$$TQ_i^{Na} = 0.378*(TQ^A/SQ^A)_{Nai} = 7.5\% \quad (5)$$

$$TQ_{ex}^{Na} = 0.622*(TQ^A/SQ^A)_{Nai} = 8.6\% \quad (6)$$

These results indicate that TQ signals in the rat head from the extracellular space could be ~ 53%. This estimation is compatible with the results of sodium TQ signal quantification performed in the rat heart (19), where it was found that extracellular TQ signal in the rat heart model can be approximately stable and is in the range of 50-64% of the total TQ signal from the normal rat heart. If in the estimation the intracellular volume is taken as 0.8 of the total tissue volume (due to CSF contribution) and sodium intracellular concentration of 10 mM, the TQ signal coming from extracellular space could be up to 73% of the total TQ signal. The significant contribution of extracellular interactions to the TQ signal is an important factor for quantification of intracellular sodium using the TQ signal.

No evidence of sodium TQ signal in samples of glycerol plus saline (1:1, v/v) is an illustration that not all binding (and short relaxation time) can yield the TQ signal. The glycerol molecule is capable to bind sodium ions and dramatically decrease sodium MR relaxation times. For example, sodium in the above mixture has relaxation times T_1 = 8.04 ± 0.06 ms and T_2 = 7.54 ± 0.04 ms at 21.1 T and room temperature. However, the tumbling time of this molecule is very short, which is not long enough to create any TQ signal (27). Such types of binding can be present *in vivo*, which decreases sodium and potassium relaxation times without detectable TQ signals (32).

Thus, the presence of fast relaxation times is not an immediate indicator of the TQ signal. The part of the fast SQ T_2 component and TQ signals may have a different origin. The TQ signal *in vivo* usually represents a specific binding which is of several ms duration, and the host molecule has a slow tumbling time which is usually provided by large molecules like proteins and DNA.

During *in vivo* investigations, changes in tissue such as pH, low oxygen can be expected to result in a new distribution of binding strength. For example, during cell death in a rat heart, a maximum TQ signal can be at the inter-pulse delay shorter than

for a normal heart (37). The deviation from an optimum TQ signal detection can be very noticeable and if not taken into consideration, it may lead to a wrong quantification. The TQTPPI pulse sequence does not have this problem. The changes in binding during interventions will be reflected by changes in the shape of the TQ signal peak, while the integral of the peak will be proportional to the amount of bound sodium. There is no need to perform an optimization of inter-pulse delay. A small tissue RF power deposition relative to the spin-lock version of the pulse sequence is another valuable benefit. No extra reference is needed as SQ signal can serve as a reference. In conclusion the ratio of TQ/SQ signals could be a very sensitive parameter to detect minor changes in binding.

For comparing the time efficiency between TQF and TQTPPI, it is important to include all the steps needed to conduct the TQF experiment. In the TQF experiments, it is necessary to find the value between the first and second RF pulses which gives the maximum TQ signal. Thus, we need to acquire a list of delays to find it. The number of delays depends on the required accuracy for this delay. Additionally, we need to acquire a SQ signal. In the TQTPPI pulse sequence all these stages are assembled together, and there is no need for any extra experiments. When the inter-pulse delay is approximately known, the number of steps in the TQTPPI can be dramatically less; for example, it can be 8. In this case TQTPPI still preserves its capability to represent changes of the TQ signal position. Thus, the actual difference in acquisition time between TQTPPI and the TQF pulse sequences may depend on the *in vivo* model we use in the TQ experiments. If the inter-pulse delay is known and we do not expect it to change during the experiments, the TQF method may take less time. However, due to filtration, the TQF technique has less sensitivity to detect small TQ signals.

Conclusion

Simultaneous detection of SQ and TQ signals using the TQTPPI method demonstrates an efficient separation of MR signals for potassium and sodium bound *in vivo* to macromolecules. The TQTPPI pulse sequence avoids the need for a separate SQ pulse sequence as it does not cancel the SQ signal, which is the case for TQF. The bound potassium and sodium signals are detected as separate peaks at the triple quantum frequency relative to the SQ signal. The experimental conditions for SQ and

TQ signals are the same which provide a high accuracy of the measurements. In comparison to the TQF methods, TQTPPI detects bound ion signals optimally for a wide range of binding strengths, which is important for evaluating ion concentration studies associated with diseases or interventions. Furthermore, the changes in sodium bindings can be monitored with an internal SQ reference signal, which is a valuable feature for *in vivo* applications. The TQ signal and its changes can be detected more sensitively, as there is no extra noise due to the filtration procedure. The quantification of the TQTPPI signals showed almost two times more effective binding of potassium than sodium, as well as a competitive binding of potassium relative to sodium for the same binding site. *In vivo* studies of the rat head showed up to ~69% of total potassium and ~27% of total sodium can be regarded as long-term bound or experience an association of several milliseconds during binding. Analysis of the results indicates that sodium ions in the extracellular space can contribute significantly to the total TQ signal. This specific feature of the TQ signals is little recognized but must be considered for studies that involve quantification of intracellular ions.

Acknowledgement

The study was performed at the National High Magnetic Field Laboratory (Tallahassee) which is supported by National Science Foundation Cooperative Agreement No. DMR-1157490 and the State of Florida. The authors thank Lothar R. Schad, Gregory S. Boebinger, Lucio Frydman and Timothy A. Cross for their support of this project. Many thanks to Steven Lee Ranner, Jason A. Kitchen, Ashley K. Blue, Richard L. Desilets, Peter L. Gor'kov and William W. Brey for the valuable and prompt help with RF probes. The authors also appreciate technical support from Shannon Helsper for help in animal handling. The authors appreciate efforts of Jacco van Beek in creation of the MatNMR software.

References

1. Yu SP, Canzoniero LM, Choi DW. Ion homeostasis and apoptosis. Current opinion in cell biology 2001;13(4):405-411.
2. Bortner CD, Cidlowski JA. Uncoupling cell shrinkage from apoptosis reveals that Na+ influx is required for volume loss during programmed cell death. J Biol Chem 2003;278(40):39176-39184.
3. Thulborn K, Lui E, Guntin J, Jamil S, Sun Z, Claiborne TC, Atkinson IC. Quantitative sodium MRI of the human brain at 9.4 T provides assessment of tissue sodium concentration and cell volume fraction during normal aging. NMR Biomed 2016;29(2):137-143.
4. Schepkin VD. Sodium MRI of glioma in animal models at ultrahigh magnetic fields. NMR Biomed 2016;29(2):175-186.
5. Madelin G, Regatte RR. Biomedical applications of sodium MRI in vivo. J Magn Reson Imaging 2013;38(3):511-529.
6. Silver IA, Deas J, Erecinska M. Ion homeostasis in brain cells: differences in intracellular ion responses to energy limitation between cultured neurons and glial cells. Neuroscience 1997;78(2):589-601.
7. Erecinska M, Dagani F. Relationships between the neuronal sodium/potassium pump and energy metabolism. Effects of K+, Na+, and adenosine triphosphate in isolated brain synaptosomes. J Gen Physiol 1990;95(4):591-616.
8. Erecinska M, Dagani F, Nelson D, Deas J, Silver IA. Relations between intracellular ions and energy metabolism: a study with monensin in synaptosomes, neurons, and C6 glioma cells. J Neurosci 1991;11(8):2410-2421.
9. Duvvuri U, Leigh JS, Reddy R. Detection of residual quadrupolar interaction in the human breast in vivo using sodium-23 multiple quantum spectroscopy. J Magn Reson Imaging 1999;9(3):391-394.
10. Reddy R, Bolinger L, Shinnar M, Noyszewski E, Leigh JS. Detection of residual quadrupolar interaction in human skeletal muscle and brain in vivo via multiple quantum filtered sodium NMR spectra. Magn Reson Med 1995;33(1):134-139.
11. Hancu I, Boada FE, Shen GX. Three-dimensional triple-quantum-filtered (23)Na imaging of in vivo human brain. Magn Reson Med 1999;42(6):1146-1154.
12. Torres AM, Philp DJ, Kemp-Harper R, Garvey C, Kuchel PW. Determination of Na+ binding parameters by relaxation analysis of selected 23Na NMR coherences: RNA, BSA and SDS. Magn Reson Chem 2005;43(3):217-224.
13. Colet JM, Bansal N, Malloy CR, Sherry AD. Multiple quantum filtered 23Na NMR spectroscopy of the isolated, perfused rat liver. Magn Reson Med 1999;41(6):1127-1135.
14. Mirkes C, Shajan G, Bause J, Buckenmaier K, Hoffmann J, Scheffler K. Triple-quantum-filtered sodium imaging at 9.4 Tesla. Magnet Reson Med 2016;75(3):1278-1289.
15. Fleysher L, Oesingmann N, Brown R, Sodickson DK, Wiggins GC, Inglese M. Noninvasive quantification of intracellular sodium in human brain using ultrahigh-field MRI. NMR Biomed 2013;26(1):9-19.
16. Petracca M, Vancea RO, Fleysher L, Jonkman LE, Oesingmann N, Inglese M. Brain intra- and extracellular sodium concentration in multiple sclerosis: a 7 T MRI study. Brain 2016;139:795-806.
17. Benkhedah N, Bachert P, Nagel AM. Two-pulse biexponential-weighted 23Na imaging. J Magn Reson 2014;240:67-76.
18. Madelin G, Lee JS, Regatte RR, Jerschow A. Sodium MRI: methods and applications. Prog Nucl Magn Reson Spectrosc 2014;79:14-47.
19. Schepkin VD, Choy IO, Budinger TF, Obayashi DY, Taylor SE, DeCampli WM, Amartur SC, Young JN. Sodium TQF NMR and intracellular sodium in isolated crystalloid perfused rat heart. Magn Reson Med 1998;39(4):557-563.

20. Rosler MB, Nagel AM, Umathum R, Bachert P, Benkhedah N. In vivo observation of quadrupolar splitting in (39) K magnetic resonance spectroscopy of human muscle tissue. NMR in biomedicine 2016;29(4):451-457.
21. Eliav U, Navon G. Sodium NMR/MRI for anisotropic systems. NMR in biomedicine 2016;29(2):144-152.
22. Eliav U, Xu X, Jerschow A, Navon G. Optic nerve: Separating compartments based on Na-23 TQF spectra and TQF-diffusion anisotropy. J Magn Reson 2013;231:61-65.
23. Marion D, Wuthrich K. APPLICATION OF PHASE SENSITIVE TWO-DIMENSIONAL CORRELATED SPECTROSCOPY (COSY) FOR MEASUREMENTS OF H-1-H-1 SPIN-SPIN COUPLING-CONSTANTS IN PROTEINS. Biochem Biophys Res Commun 1983;113(3):967-974.
24. Ernst RR, Bodenhausen G, Wokaun A. Principles of nuclear magnetic resonance in one and two dimensions. Oxford Oxfordshire
New York: Clarendon Press ;
Oxford University Press; 1987. xxiv, 610 p. p.
25. Van der Maarel JRC. Thermal relaxation and coherence dynamics of spin 3/2. I. Static and fluctuating quadrupolar interactions in the multipole basis. Concept Magn Reson A 2003;19A(2):97-116.
26. Van der Maarel JRC. RELAXATION OF SPIN QUANTUM NUMBER S=3/2 UNDER MULTIPLE-PULSE QUADRUPOLAR ECHOES. J Chem Phys 1991;94(7):4765-4775.
27. Schepkin VD, Gawlick U, Ross BD, Chenevert TL. Detection of triple quantum Na NMR in normal and tumored mouse brain. Proceedings, 11th Annual Meeting, ISMRM, p 39. Volume 11. Toronto, Canada; 2003. p 39.
28. Nagel AM, Umathum R, Rosler MB, Ladd ME, Litvak I, Gor'kov PL, Brey WW, Schepkin VD. (39) K and (23) Na relaxation times and MRI of rat head at 21.1 T. NMR Biomed 2016;29(6):759-766.
29. Gor'kov PL, Qian C, Beck BL, Clark M, Masad IS, Schepkin VD, Grant SC, Brey WW. A modular MRI probe for large rodent neuroimaging at 21.1 T (900 MHz). Proceeding, 17th Annual Meeting, ISMRM, p 2952. Honolulu, Hawai'i, USA; 2009.
30. van Beek JD. matNMR: A flexible toolbox for processing, analyzing and visualizing magnetic resonance data in Matlab((R)). J Magn Reson 2007;187(1):19-26.
31. Jaccard G, Wimperis S, Bodenhausen G. Multiple-Quantum Nmr-Spectroscopy of S=3/2 Spins in Isotropic-Phase - a New Probe for Multiexponential Relaxation. J Chem Phys 1986;85(11):6282-6293.
32. Rooney WD, Springer CS, Jr. A comprehensive approach to the analysis and interpretation of the resonances of spins 3/2 from living systems. NMR Biomed 1991;4(5):209-226.
33. Abragam A. The principles of nuclear magnetism. Oxford,: Clarendon Press; 1961. 599 p. p.
34. Kurland R, Newton C, Nir S, Papahadjopoulos D. SPECIFICITY OF NA+ BINDING TO PHOSPHATIDYLSERINE VESICLES FROM NA-23 NMR RELAXATION RATE STUDY. Biochim Biophys Acta 1979;551(1):137-147.
35. Sanui H, Pace N. SODIUM AND POTASSIUM BINDING BY RAT LIVER CELL MICROSOMES. Journal of General Physiology 1959;42(6):1325-1345.
36. Thulborn KR, Davis D, Adams H, Gindin T, Zhou J. Quantitative tissue sodium concentration mapping of the growth of focal cerebral tumors with sodium magnetic resonance imaging. Magn Reson Med 1999;41(2):351-359.
37. Schepkin VD, Choy IO, Budinger TF. Sodium alterations in isolated rat heart during cardioplegic arrest. J Appl Physiol 1996;81(6):2696-2702.